<u>Combined Analysis</u>: Texture-structure-microstructure-phase analysis of multi-phased ceramics and films using x-ray and neutron diffraction: examples of sinter-forged Bi2223-Bi2212, Melt Textured Growth Y-Ba-Cu-O and nano-Si

Daniel Chateigner

CRISMAT-ENSICAEN (Caen-France)

Jesus Ricote

DMF-CSIC (Madrid-Spain)

High-Tc Superconductors

nano-Si thin films

PCT & PMN-PT Ferroelectrics

Electroceramics X, Toledo 2006

Implemented codes

Extracted Intensities

WIMV, E-WIMV
Harmonics, components, ADC, arbitrary

Orientation Distribution Function

Rietveld

Structure
+
Microstructure
+
phase %

Popa-Balzar,
$sin^2\psi$

Residual stresses
Strain Distribution Function

Geometric mean, Reuss, Voigt, Hill

Le Bail

Specular Reflectivity

Roughness,
electron Density
& EDP,
Thickness

Fresnel,
Matrix (Parrat),
DWBA

pole figures
inverse pole figures

Structural parameters
atomic positions, substitutions, vibrations
cell parameters

Multiphased, layered samples:
Thickness,
Anisotropic Sizes
and μ−strains (*Popa*),
Stacking faults (*Warren*),
Distributions

Phase ratio (amorphous + crystalline)
Le Bail *Rietveld*

Texture from Spectra

Orientation Distribution Function (ODF)

From pole figures

From spectra

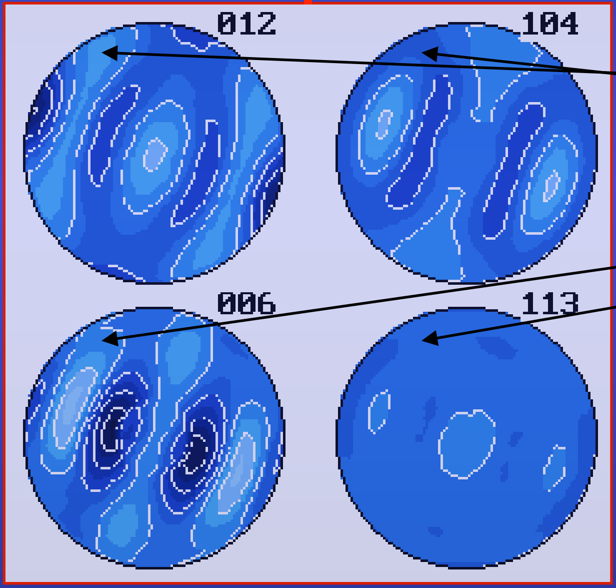

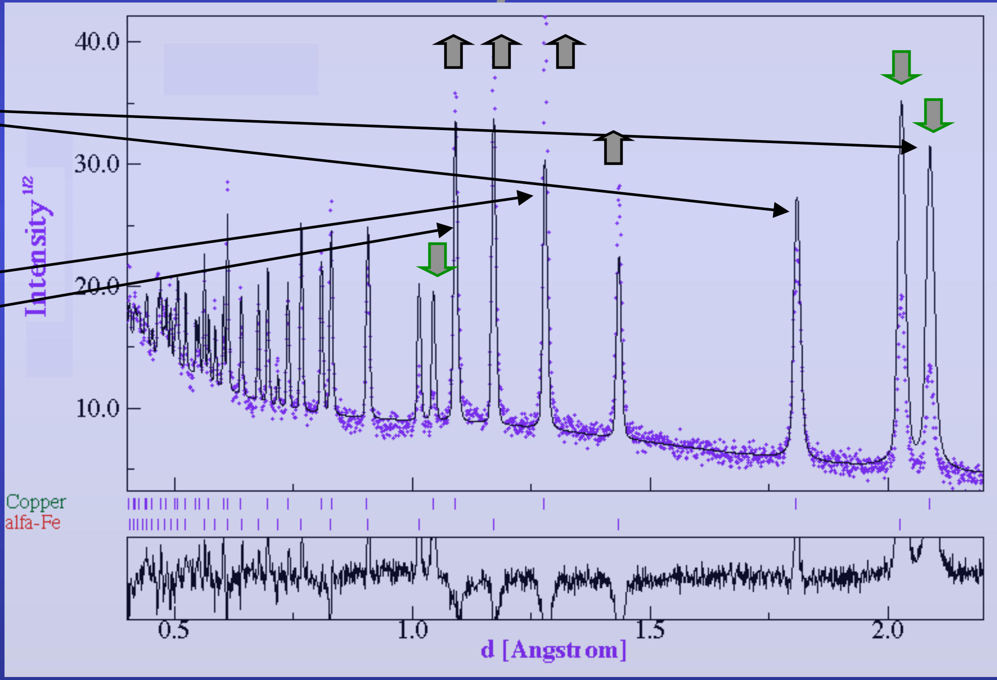

Residual Stresses and Rietveld

- Macro elastic strain tensor (I kind)
- Crystal anisotropic strains (II kind)

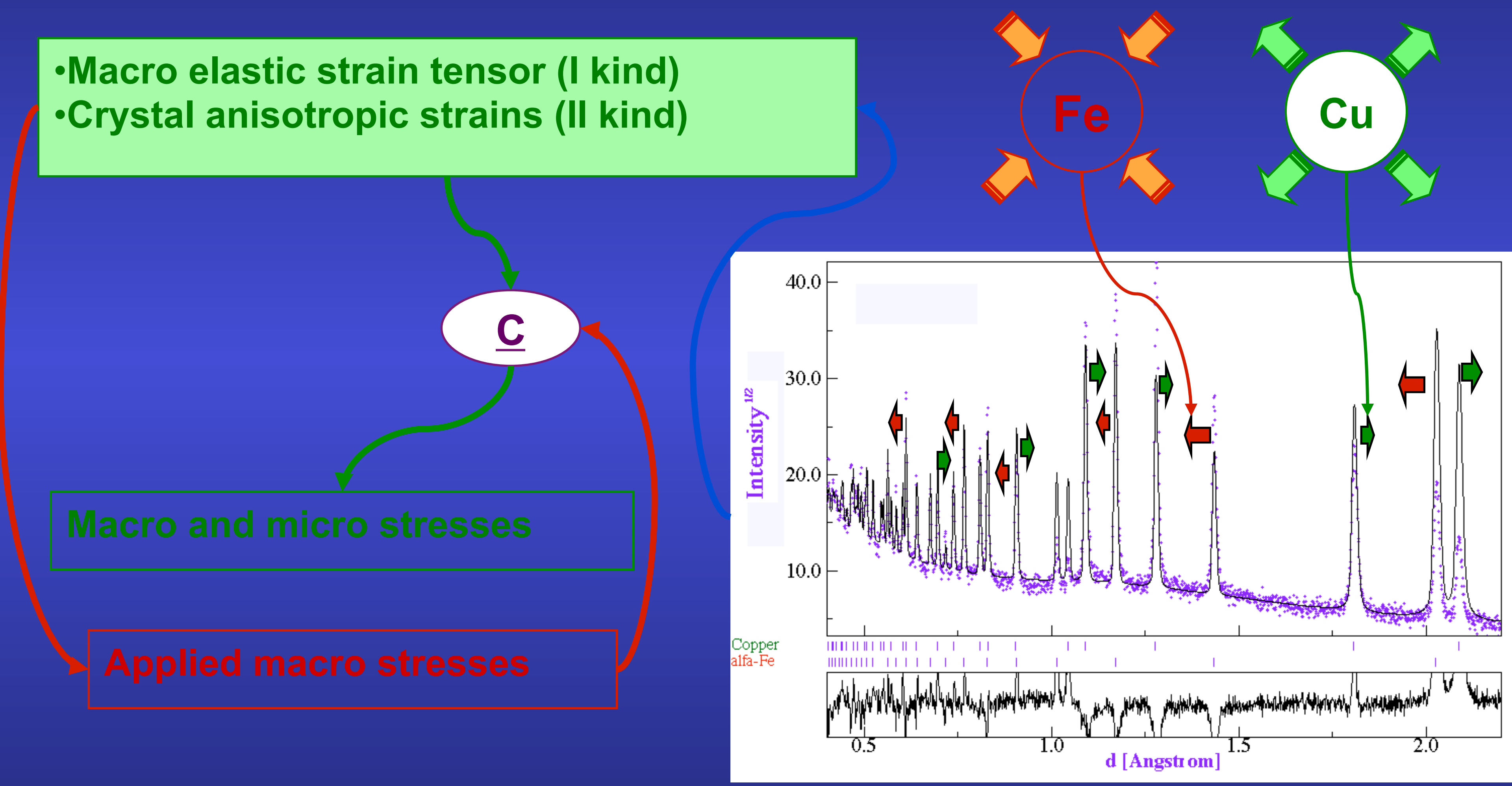

Textured samples: Reuss, Voigt, Hill, Bulk geometric mean approaches

How it works (Combined)

$$I_i^{calc}(\chi,\phi) = \sum_{n=1}^{Nphases} S_n \sum_k L_k \left|F_{k;n}\right|^2 S\left(2\theta_i - 2\theta_{k;n}\right) P_{k;n}(\chi,\phi) A + bkg_i$$

Texture

$$P_k(\chi,\phi) = \int_{\varphi} f(g,\varphi)\, d\varphi$$

- from Generalized Spherical Harmonics:

$$P_k(\chi,\phi) = \sum_{l=0}^{\infty} \frac{1}{2l+1} \sum_{n=-l}^{l} k_l^n(\chi,\phi) \sum_{m=-l}^{l} C_l^{mn} k_n^{*m}(\Theta_k \phi_k)$$

$$f(g) = \sum_{l=0}^{\infty} \sum_{m,n=-l}^{l} C_l^{mn} T_l^{mn}(g)$$

- from the WIMV (left) iterative process or entropy maximisation (right):

$$f^{n+1}(g) = N_n \frac{f^n(g) f^0(g)}{\left(\prod_{\mathbf{h}=1}^{I} \prod_{m=1}^{M_\mathbf{h}} P_\mathbf{h}^n(\mathbf{y}) \right)^{\frac{1}{IM_\mathbf{h}}}}$$

$$f^{n+1}(g) = f^n(g) \prod_{m=1}^{M_\mathbf{h}} \left(\frac{P_\mathbf{h}(\mathbf{y})}{P_\mathbf{h}^n(\mathbf{y})} \right)^{\frac{r_\mathbf{n}}{M_\mathbf{h}}}$$

Layering

$$C_\chi^{\text{top film}} = g_1\left(1-\exp\left(-\mu T g_2/\cos\chi\right)\right)/\left(1-\exp\left(-2\mu T/\sin\omega\cos\chi\right)\right)$$

$$C_\chi^{\text{cov. layer}} = C_\chi^{\text{top film}}\left(\exp\left(-g_2\sum\mu_i^{'}T_i^{'}/\cos\chi\right)\right)/\left(\exp\left(-2\sum\mu_i^{'}T_i^{'}/\sin\omega\cos\chi\right)\right)$$

Popa anisotropic shapes & microstrains

$$\langle R_{\mathbf{h}}\rangle = R_0 + R_1P_2^{\,0}(x) + R_2P_2^{\,1}(x)\cos\varphi + R_3P_2^{\,1}(x)\sin\varphi + R_4P_2^{\,2}(x)\cos2\varphi + R_5P_2^{\,2}(x)\sin2\varphi + \ldots$$

$$\langle\varepsilon_{\mathbf{h}}^{\,2}\rangle E_{\mathbf{h}}^{\,4} = E_1h^4 + E_2k^4 + E_3\ell^4 + 2E_4h^2k^2 + 2E_5\ell^2k^2 + 2E_6h^2\ell^2 + 4E_7h^3k + 4E_8h^3\ell + 4E_9k^3h + 4E_{10}k^3\ell + 4E_{11}\ell^3h + 4E_{12}\ell^3k + 4E_{13}h^2k\ell + 4E_{14}k^2h\ell + 4E_{15}\ell^2kh$$

Roughness and/or microabsorption

$$R^{rough}\left(q_z\right) = R\left(q_z\right)\exp(-q_{z,0}q_{z,1}\sigma^2)$$ Low-angles (reflectivity)

$$S_R = 1-p\exp\left(-q\right) + \mathrm{p}\exp\left(\frac{-\mathrm{q}}{\sin\theta}\right)$$ high-angle (Suortti)

Specular reflectivity: **q**=(0,0,z)

- Fresnel:

$$R(\mathbf{q}) = \left| \frac{q_z - \sqrt{q_z^2 - q_c^2 + \frac{32 i \pi^2 \beta}{\lambda^2}}}{q_z + \sqrt{q_z^2 - q_c^2 + \frac{32 i \pi^2 \beta}{\lambda^2}}} \right|^2 \delta q_x \delta q$$

- matrix:

$$R^{flat} = \frac{r_{0,1}^2 + r_{1,2}^2 + 2 r_{0,1} r_{1,2} \cos 2 k_{Z,1} h}{1 + r_{0,1}^2 r_{1,2}^2 + 2 r_{0,1} r_{1,2} \cos 2 k_{Z,1} h}$$

- Born approximation:

$$R(q_z) = r.r^* = R_F(q_z) \left| \frac{1}{\rho_s} \int_{-\infty}^{+\infty} \frac{d\rho(z)}{dz} e^{i q_z z} dz \right|^2$$

Phase

$$W_{\Phi} = \frac{S_{\Phi} Z_{\Phi} M_{\Phi} V_{\Phi}}{\sum_{i=1}^{N_{\Phi}} S_i Z_i M_i V_i}$$

Strain-Stress

$$\boldsymbol{\varepsilon}(\mathbf{X}) = \boldsymbol{\varepsilon}^{\mathrm{I}} + \boldsymbol{\varepsilon}^{\mathrm{II}}(\mathbf{X}) + \boldsymbol{\varepsilon}^{\mathrm{III}}(\mathbf{X})$$

$$\begin{aligned}\langle \varepsilon_{\mathrm{h}}(\mathbf{y}) \rangle_{V_d} &= \frac{1}{V_d} \int_{V_d} (\varepsilon_{33}^{I} + \varepsilon_{33}^{II} + \varepsilon_{33}^{III}) dV \\ &= (\varepsilon_{11}^{I} \cos^2\phi + \varepsilon_{12}^{I} \sin 2\phi + \varepsilon_{22}^{I} \sin^2\phi - \varepsilon_{33}^{I}) \sin^2\psi + \varepsilon_{33}^{I} + \\ &(\varepsilon_{13}^{I} \cos\phi + \varepsilon_{23}^{I} \sin\phi) \sin 2\psi + \frac{1}{V_d} \int_{V_d} (\varepsilon_{33}^{IIe} + \varepsilon_{33}^{IIti} + \varepsilon_{33}^{IIpi}) dV \\ &= \frac{\langle d(hkl,\phi,\psi) \rangle_{V_d} - d_0(hkl)}{d_0(hkl)}\end{aligned}$$

Isotropic samples:
Tri-, bi-, uni-axial stress states

Textured samples:
Tri-, bi-, uni- stress states
+ ODF + SDF + model

$$\langle E(\mathbf{g}) \rangle_{V_d} = \frac{1}{V_d} \int_{V_d} E^{SC}(g) f(g) dg \quad \Rightarrow \quad \mathrm{C}_{\mathrm{ijkl}}^{\mathrm{M}} \neq \left(\mathrm{S}_{\mathrm{ijkl}}^{\mathrm{M}}\right)^{-1}$$

$$= \left(\prod_{V_d} E^{SC}(g) f(g) dg \right)^{\frac{1}{V_d}} \quad \Rightarrow \quad \mathrm{C}_{\mathrm{ijkl}}^{\mathrm{M}} = \left(\mathrm{S}_{\mathrm{ijkl}}^{\mathrm{M}}\right)^{-1}$$

Reuss, Voigt, Hill

Geometric mean, *VPSC*

Minimum experimental requirements

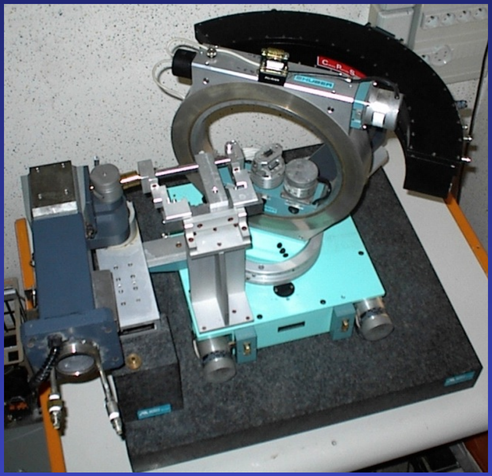

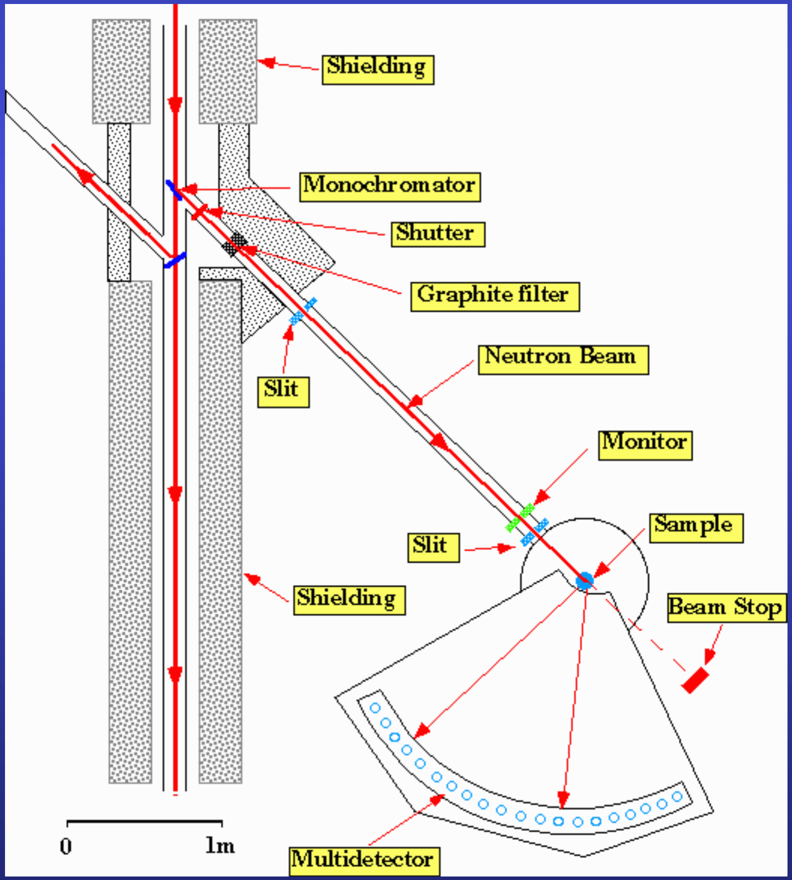

1D or 2D Detector + 4-circle diffractometer
(X-rays and neutrons)
CRISMAT, ILL

+

~1000 experiments (2θ diagrams)
in as many sample orientations

+

Instrument calibration
(peaks widths and shapes,
misalignments, defocusing …)

Calibration

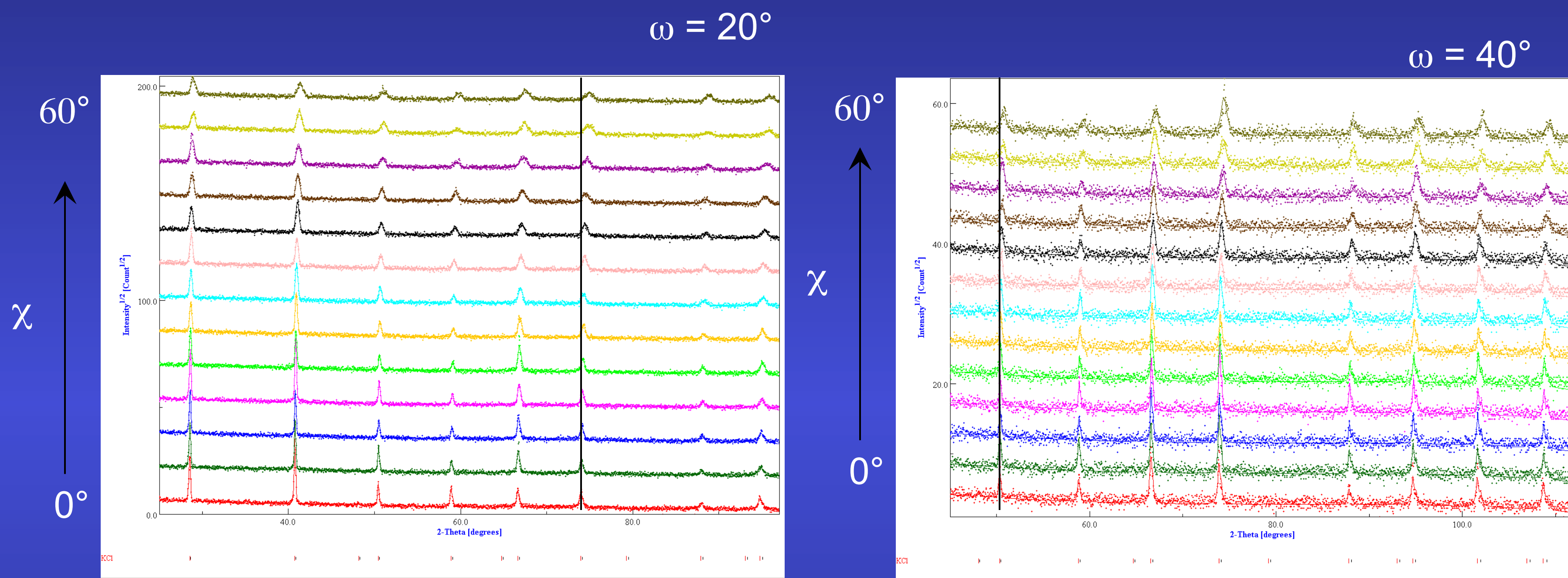

KCl, LaB_6 …

FWHM (ω, χ, 2θ …)
2θ shift
gaussianity
asymmetry
misalignments ...

Methodology implementation

L. Lutterotti, Trento

User friendly interface

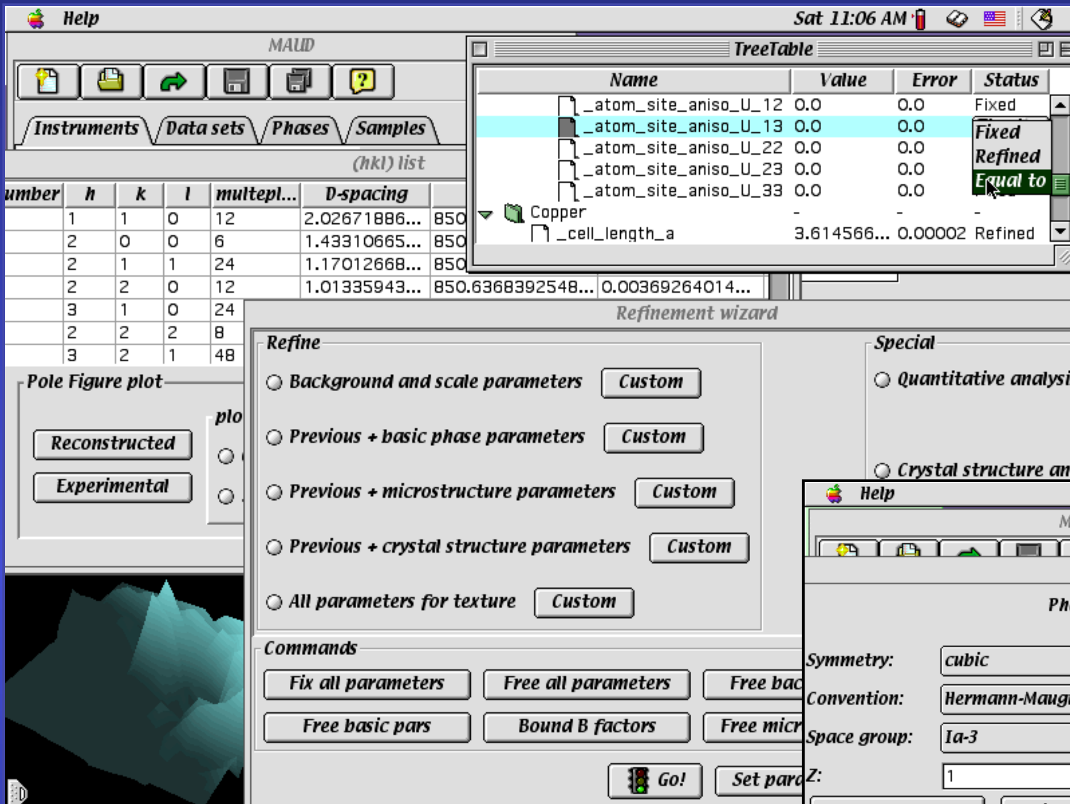

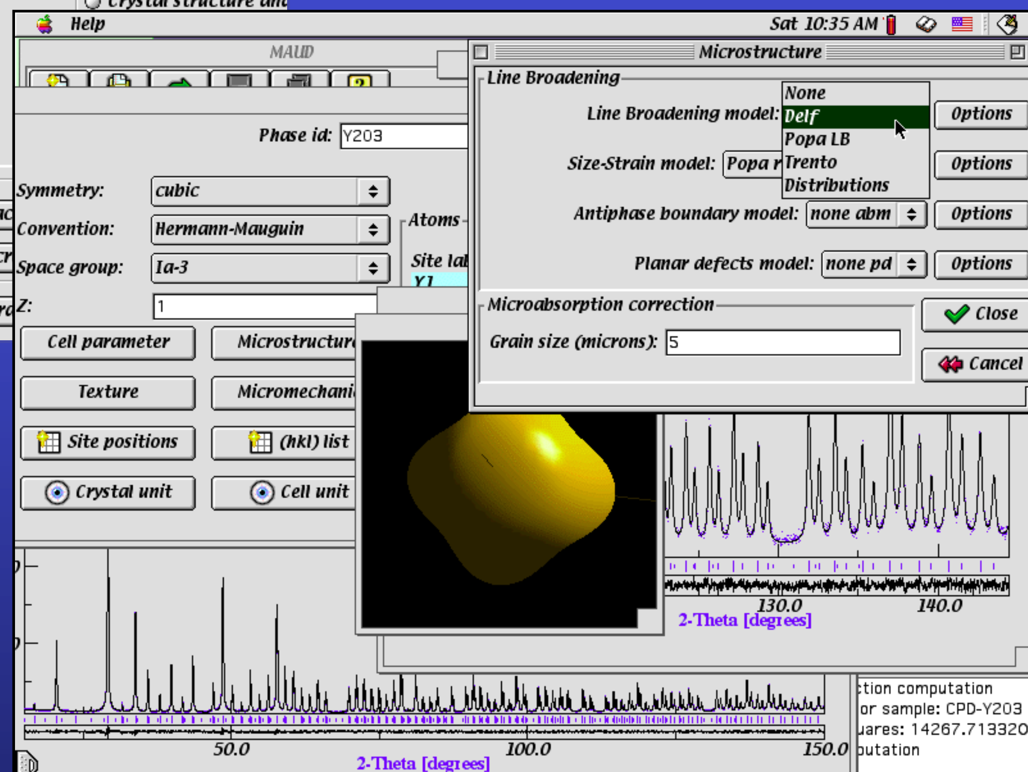

Java codes

Java web start updates

Bi2223 compounds

E. Guilmeau, CRISMAT

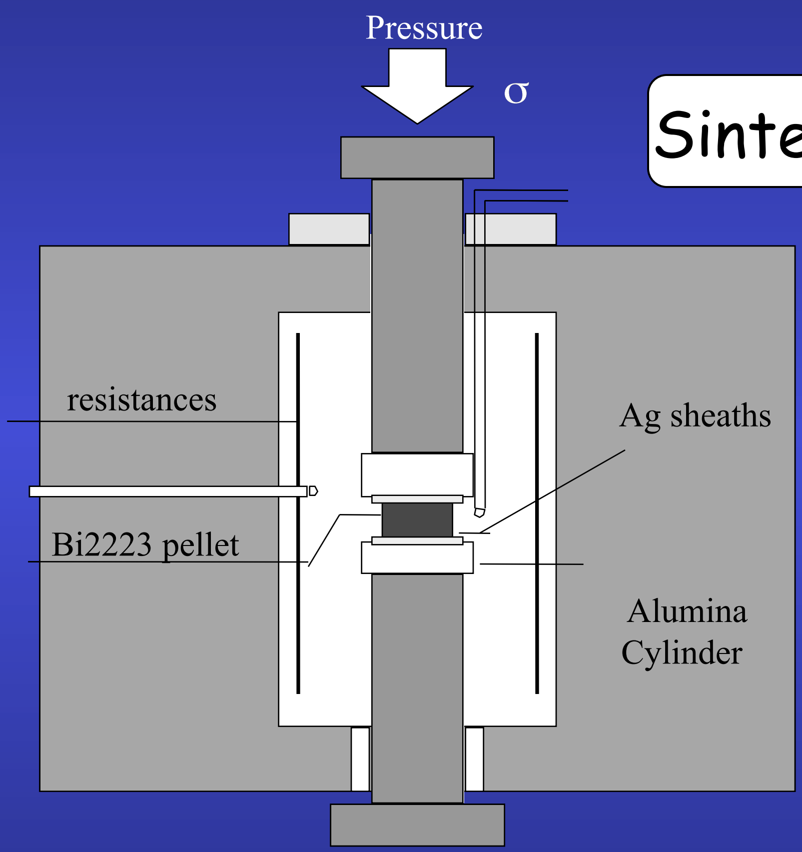

Sinter-Forging

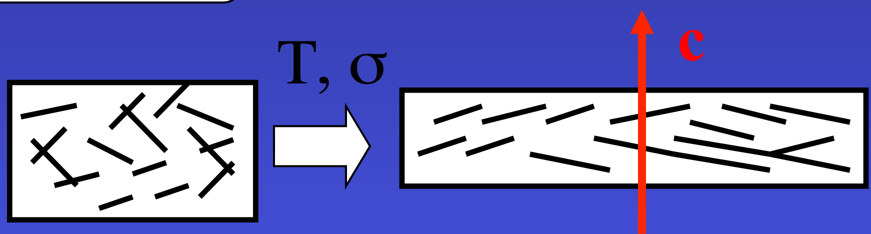

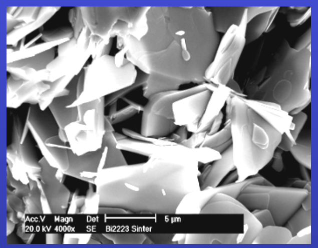

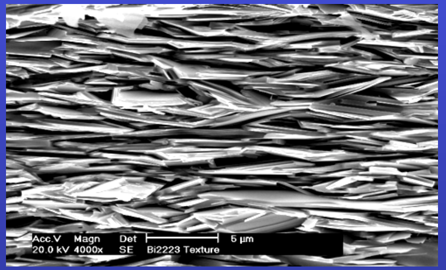

Grain alignment ⇒ ↗ Jc

(00ℓ) Texture

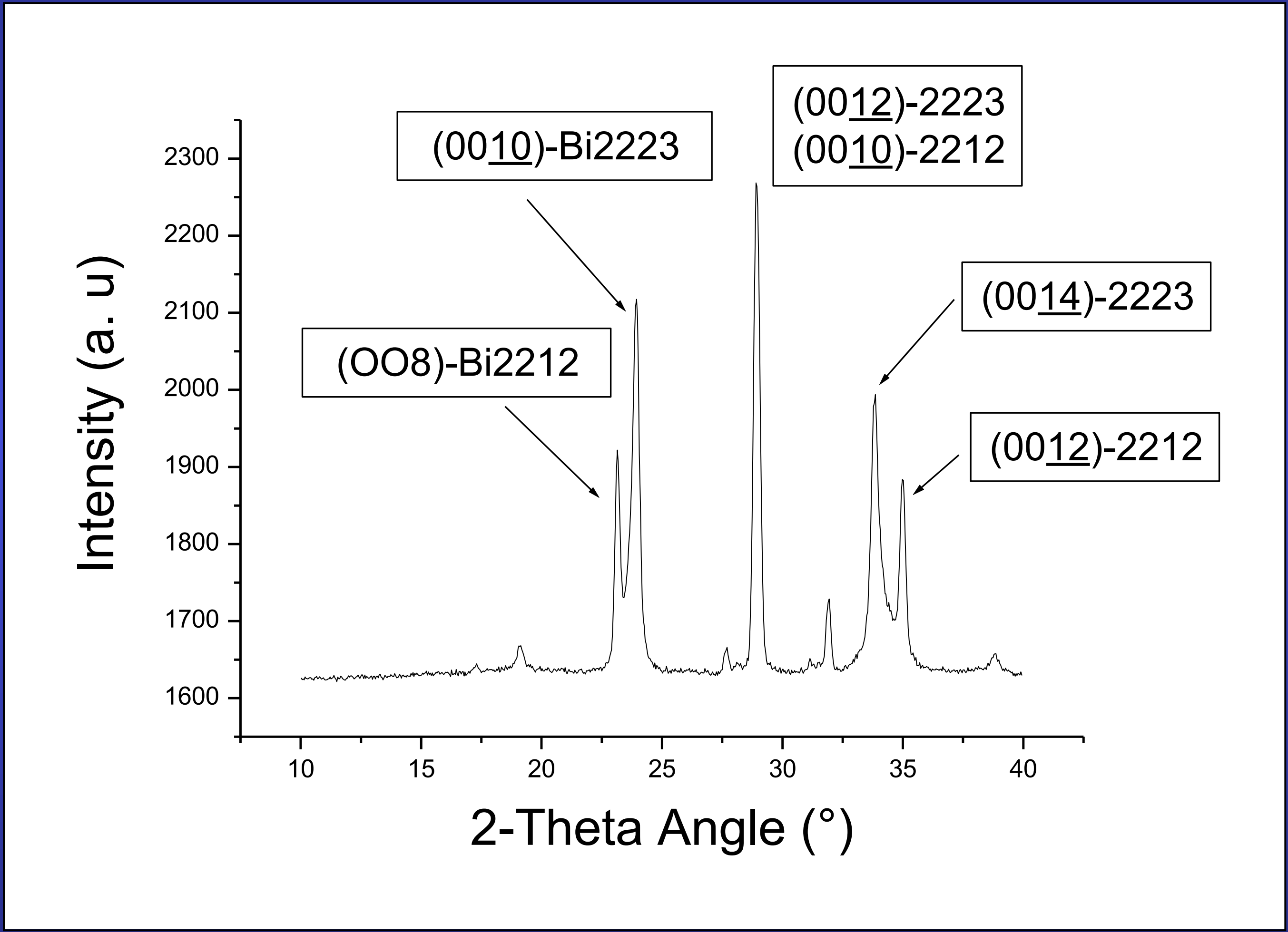

(0010)-Bi2223
(0012)-2223
(0010)-2212
(0014)-2223
(OO8)-Bi2212
(0012)-2212
Intensity (a. u)
2300
2200
2100
2000
1900
1800
1700
1600
10
15
20
25
30
35
40
2-Theta Angle (°)

Bi2212 + Secondary phases ⟶ Bi2223

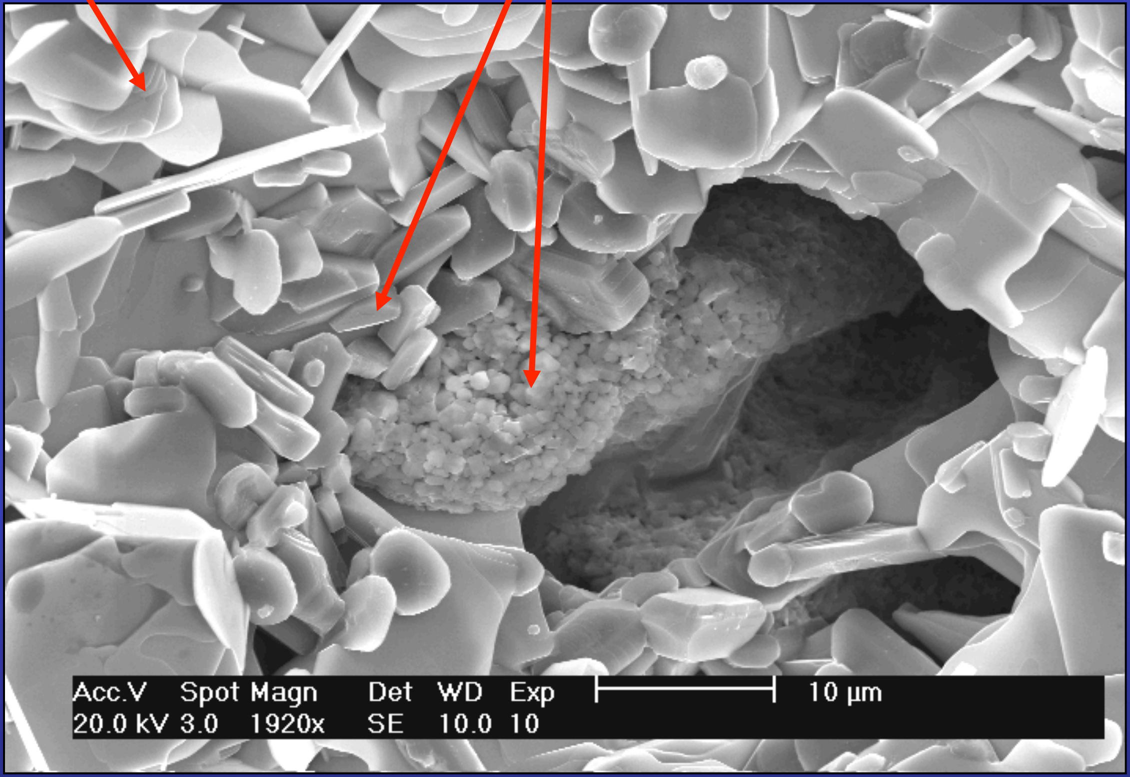

Combined Analysis

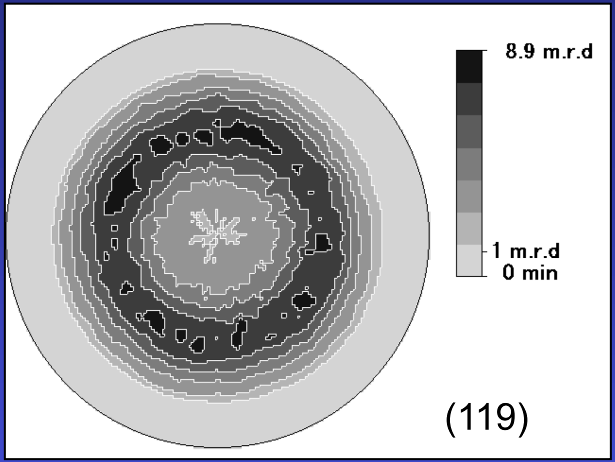

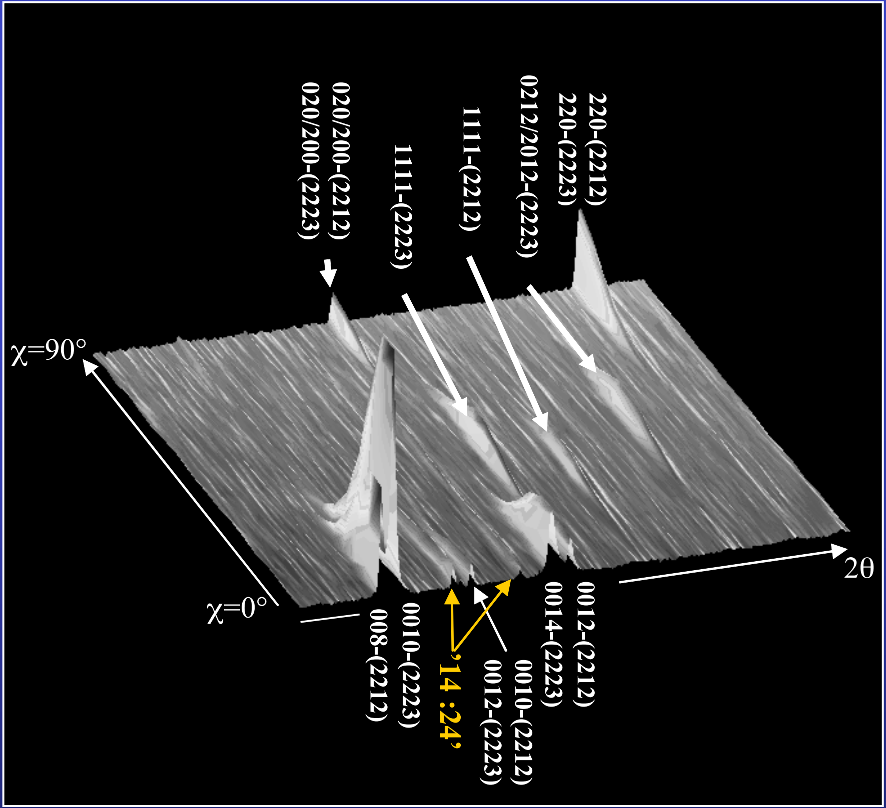

- *Neutrons*
- Sample: ~70 mm^3
- 2θ patterns for χ=0° to 90°
- No φ rotation (fibre texture).

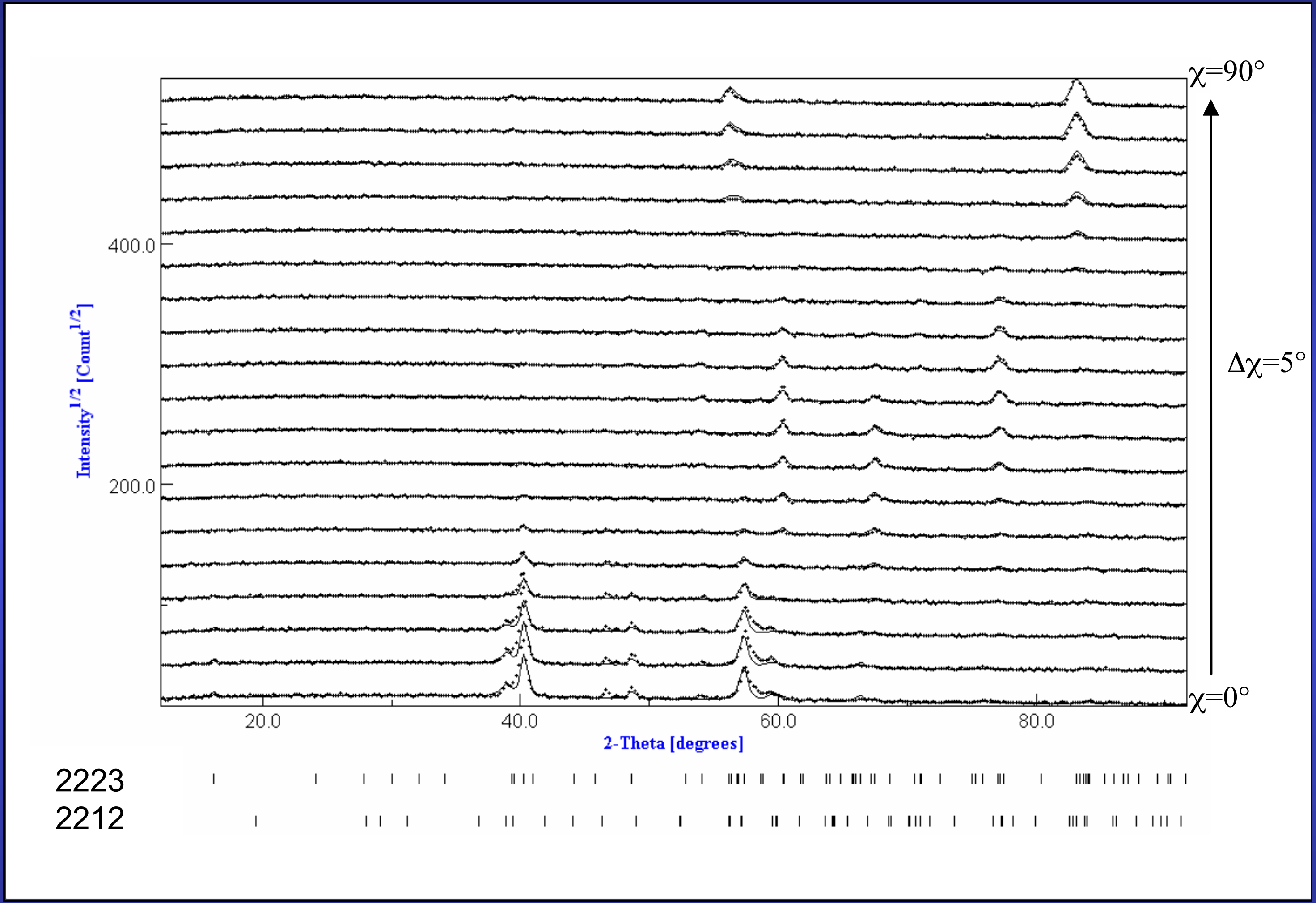

Rw=9.12
RP=16.24

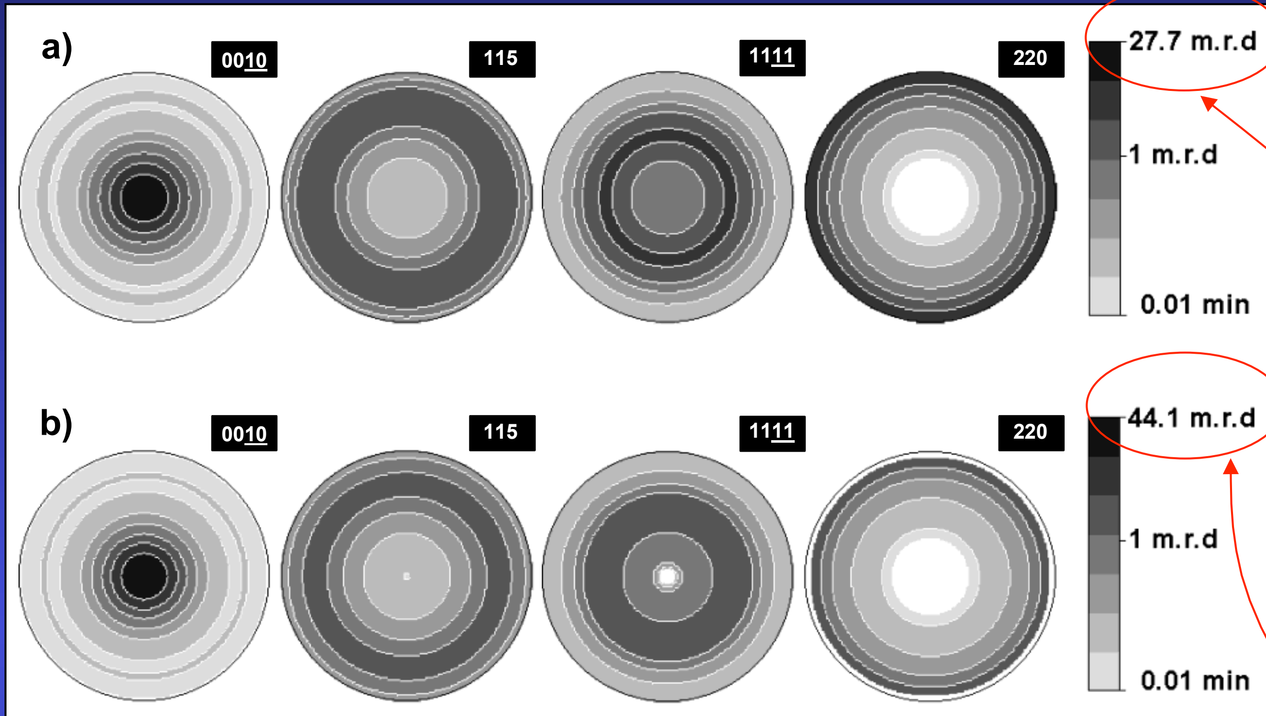

Logarithmic density scale, equal area projection

Recalculated (WIMV)

Extracted (Le Bail)

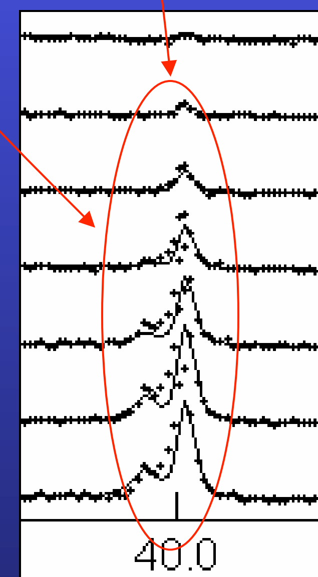

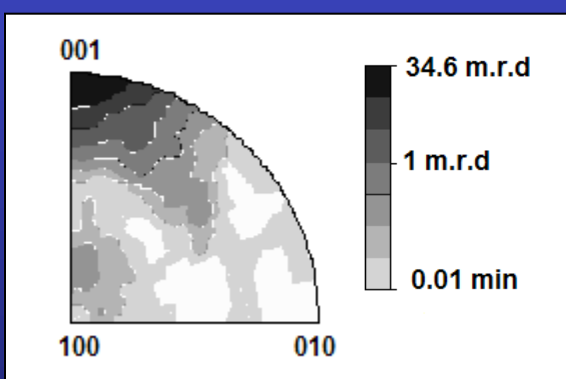

Logarithmic density scale, equal area projection

Stacking faults and/or intergrowth on the c-axis →New periodicities and peaks characterized with intermediate c parameters.

However, no algorithm is included to solve intergrowths in the combined approach.

Effect of the sinter-forging treatment on the texture development, crystal growth, transport properties

Sinter-forging dwell time (h)	*Orientation Distribution Max (m.r.d.)*		*% Bi2223*	*Cell parameters (Å)*		*Crystallite size Bi2223 (nm)*	*Rb (%)*	*Rw (%)*	*Rexp (%)*	*RP0 (%)*	*RP1 (%)*	*J_c (A/cm^2)*
	Bi2212	*Bi2223*		*Bi2223*	*Bi2212*							
20	21.8	20.7	59.9±1.3	a=5.419(3) b=5.391(3) c=37.168(3)	a=5.414(3) b=5.393(3) c=30.800(3)	205±7	7.56	11.1	4.55	17.74	10.56	12500
50	24.1	24.4	72.9±2.9	a=5.419(3) b=5.408(3) c=37.192(3)	a=5.416(3) b=5.396(3) c=30.806(3)	273±10	7.54	11.37	4.58	17.05	11.04	15000
100	31.5	25.2	84.4±4.6	a=5.410(3) b=5.405(3) c=37.144(3)	a=5.412(3) b=5.403(3) c=30.752(3)	303±10	5.4	8.04	3.69	13.54	9.31	19000
150	65.4	27.2	87.0±4.1	a=5.417(3) b=5.403(3) c=37.199(3)	a=5.413(3) b=5.407(3) c=30.792(3)	383±13	6.13	9.12	4.8	16.24	12.25	20000

↗ *Sinter-forging Time* ⇒ ↗ Texture strength, ↗ % Bi2223, ↗ Crystallite Size ⇔ ↗ J_c

Model ?

E. Guilmeau et al., JAC

$YBa_2Cu_3O_{7+d}$ compounds

D. Grossin, S. Meslin, CRISMAT

MTG, TSMTG, infiltrated/perforated and foams

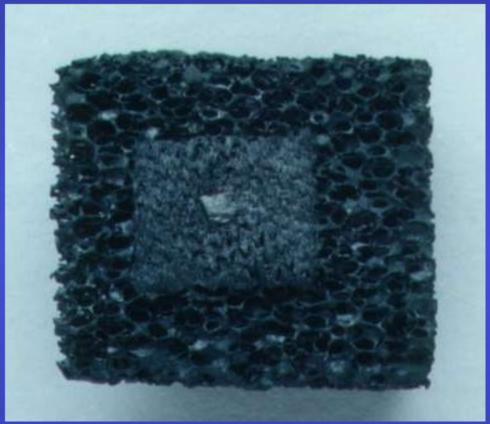

Infiltrated Polyurethane foam, annealed

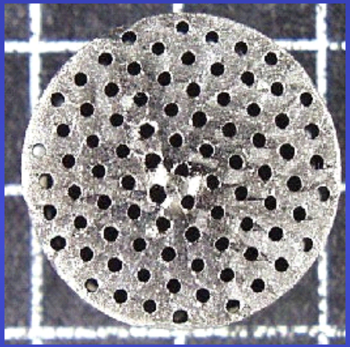

Perforated

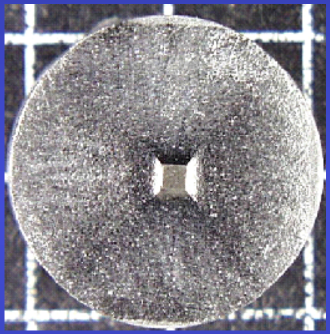

TSMTG

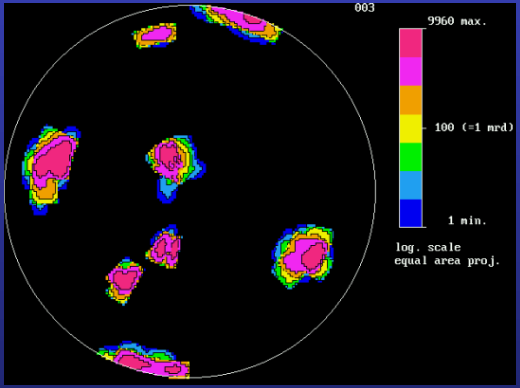

Mixtures of YBa2Cu3O7 superconducting and Y2BaCuO5 insulating (needed for vortex pinning)

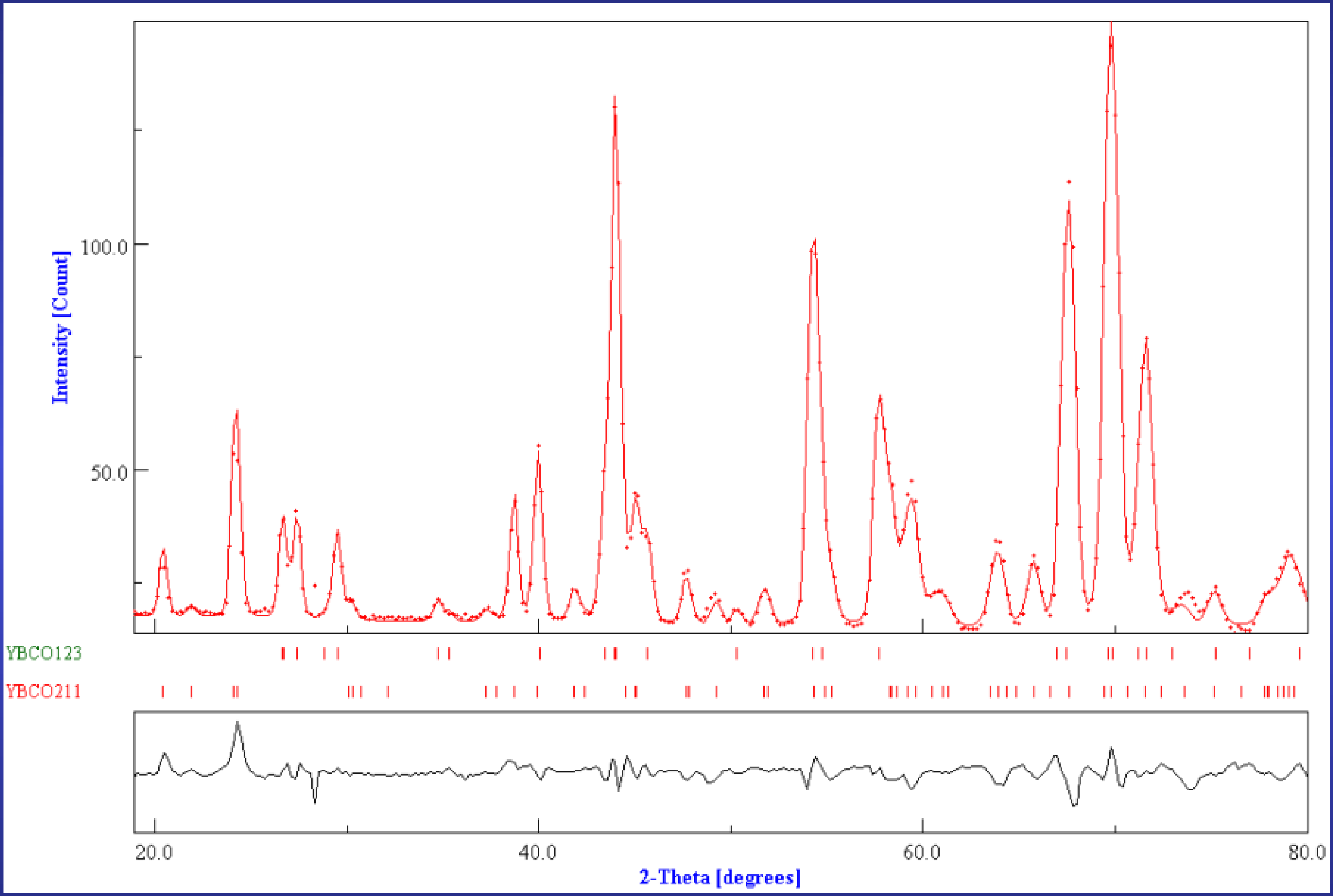

$R_w = 5.43\%$, $R_{Bragg} = 19.71\%$

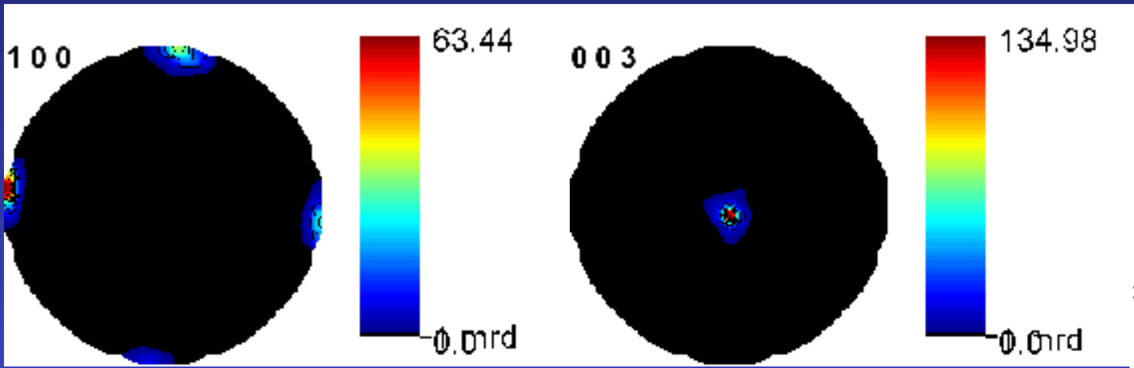

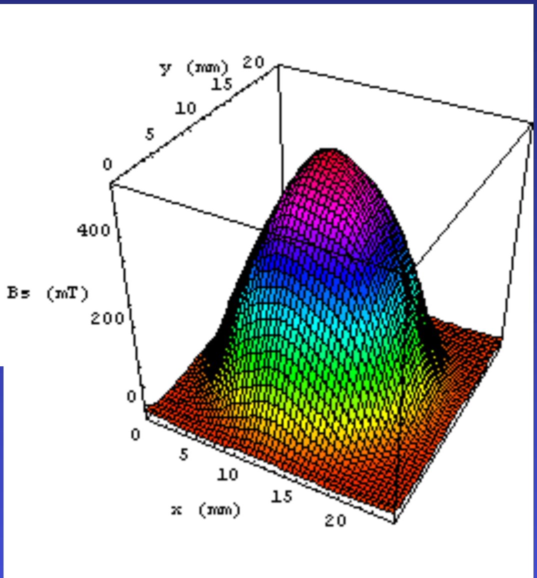

Neutron pole figures (D1B-ILL) and trapped flux

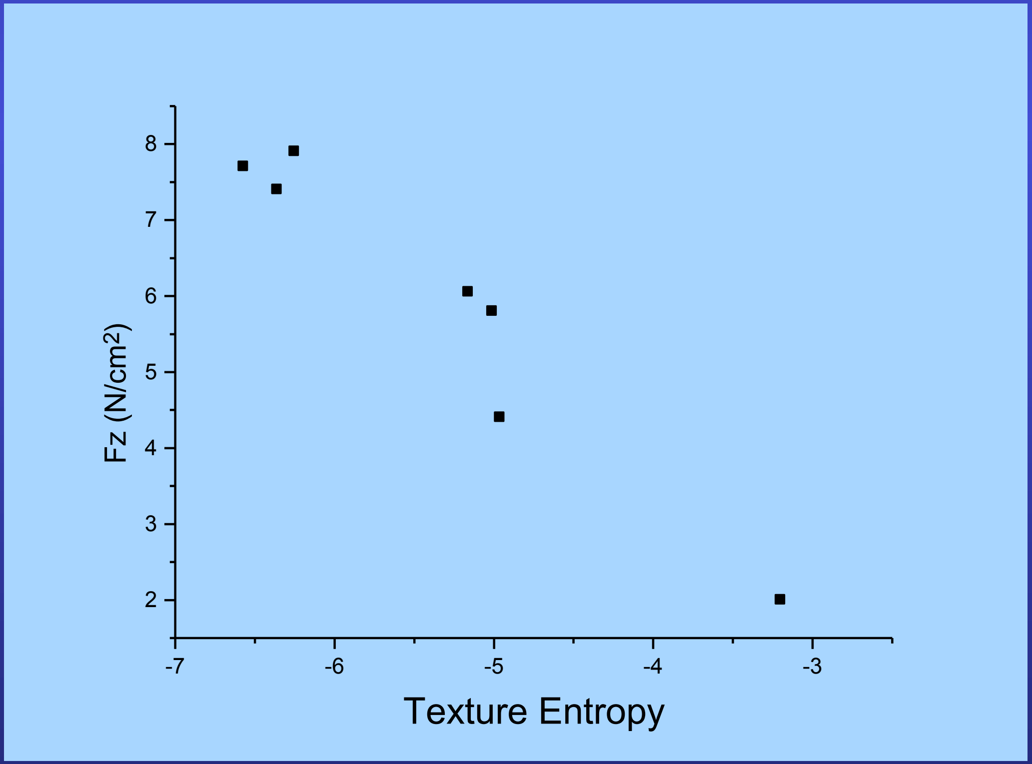

Levitation force

Models ?

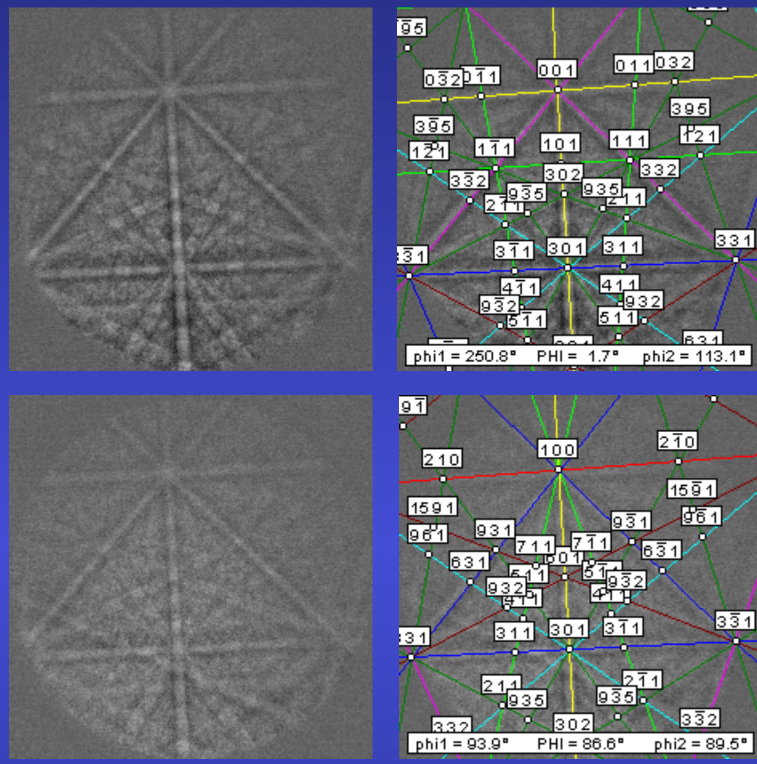

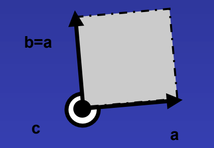

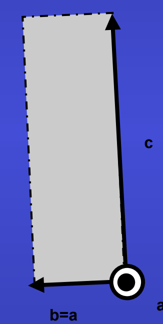

Scan 01
(1.42% 90-misorientation)

Scan 02
(1.66% 90-misorientation)

Scan 03
(1.59% 90-misorientation)

Scan SUM

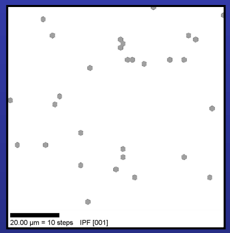

+

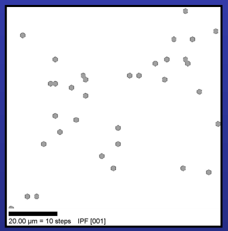

+

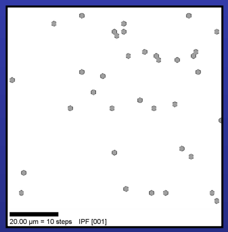

=

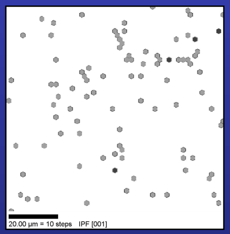

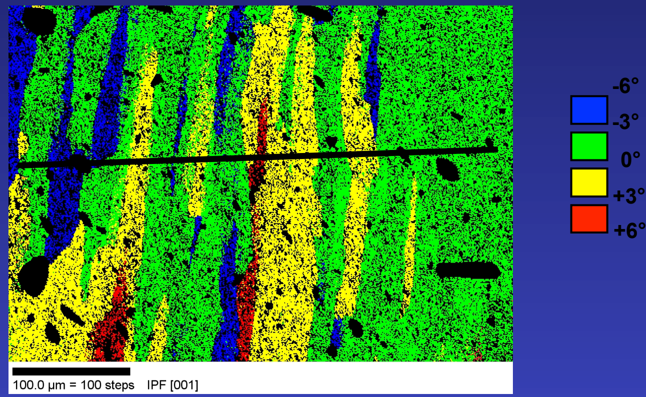

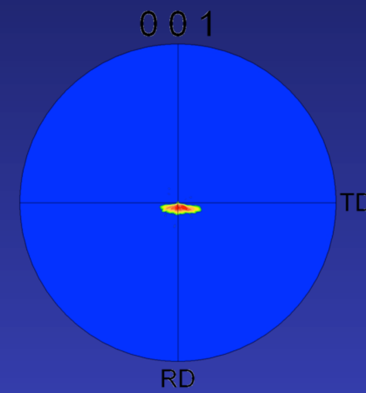

EBSD {001}:
max = 1600 mrd

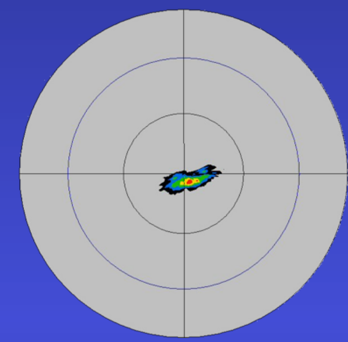

ND {001}: max = 128 mrd

EBSD rescaling ?

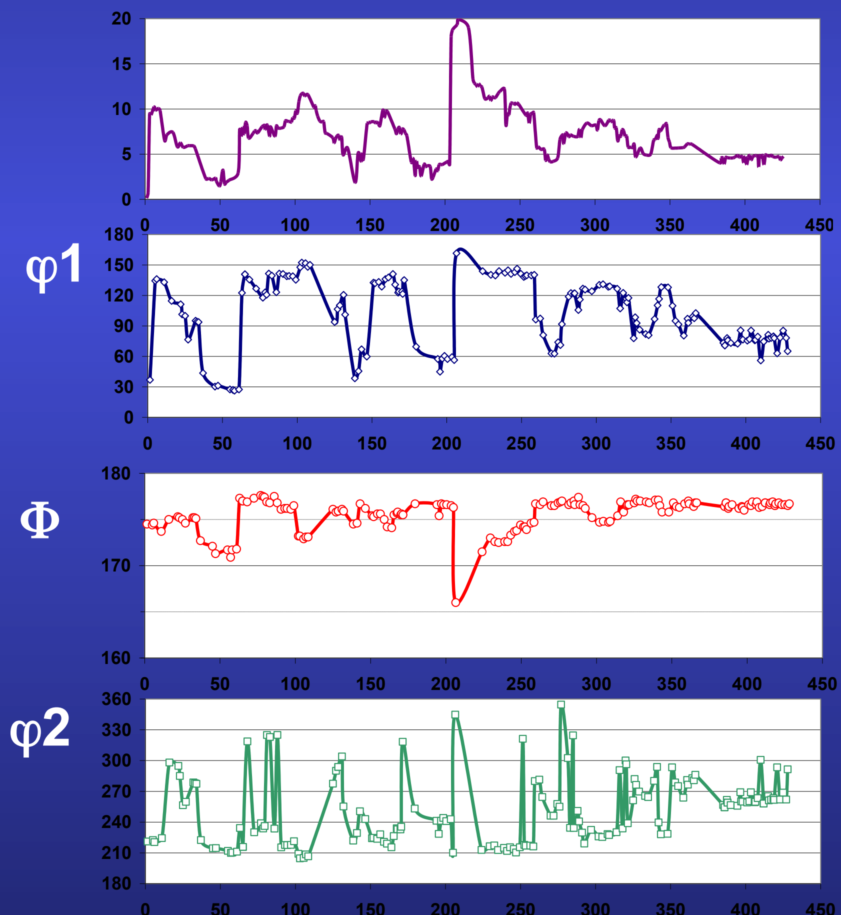

- Small g variation inside on twinned domain: large Jc's

- large φ_1 variations at twin boundaries: Twist boundaries

- but small Φ variations: small tilt boundaries: large Jc's too

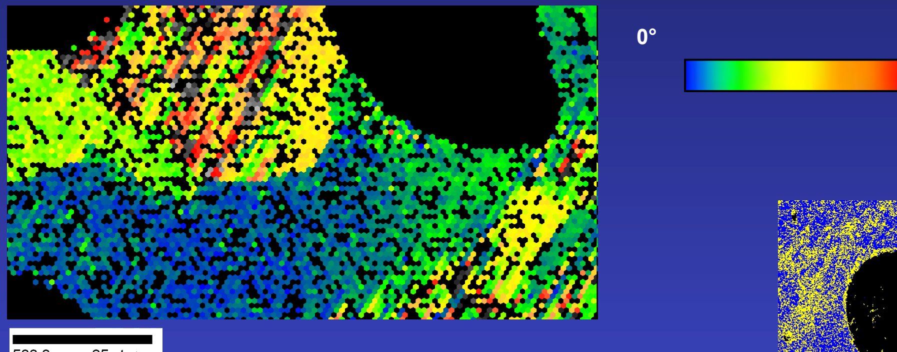

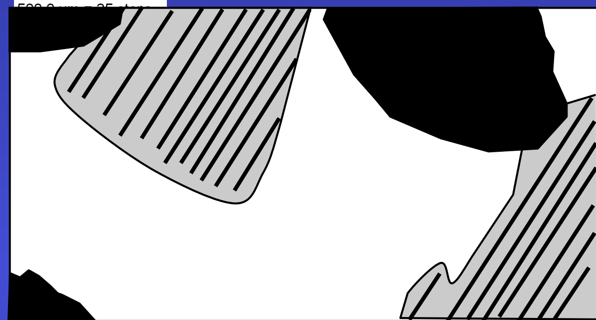

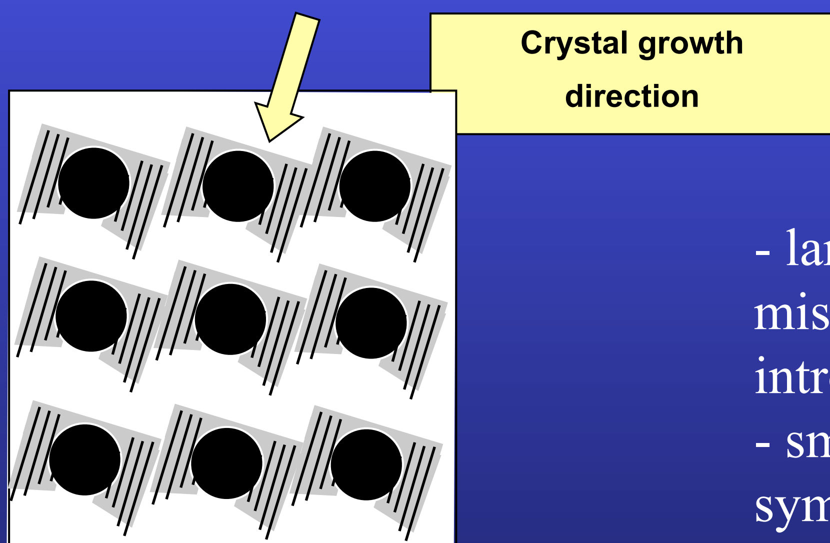

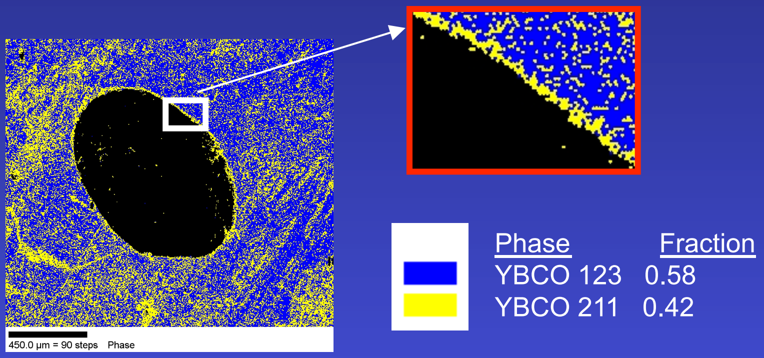

- large and small subdomains misorientation are observed, introduced by perforation
- small dg accessible in pseudo-symmetry

Si nanocrystalline thin films

M. Morales, SIFCOM-Caen

Silicon thin films deposition by reactive magnetron sputtering:

- power density 2W/cm^2
- total pressure: $p_{total} = 10^{-1}$ Torr
- plasma mixture: H_2 / Ar, pH_2 / p_{total} = 80 %
- temperature: 200°C
- substrates: amorphous SiO_2 (a-SiO_2)
  (100)-Si single-crystals
- target-substrate distance (d)
  - a-SiO_2 substrates: d = 4, 6, 7, 8, 10, 12 cm
    films A, B, C, D, E, F
  - (100)-Si: d = 6, 12 cm
    films G, H

Aim: quantum confinement, photoluminescence properties

Isotropic

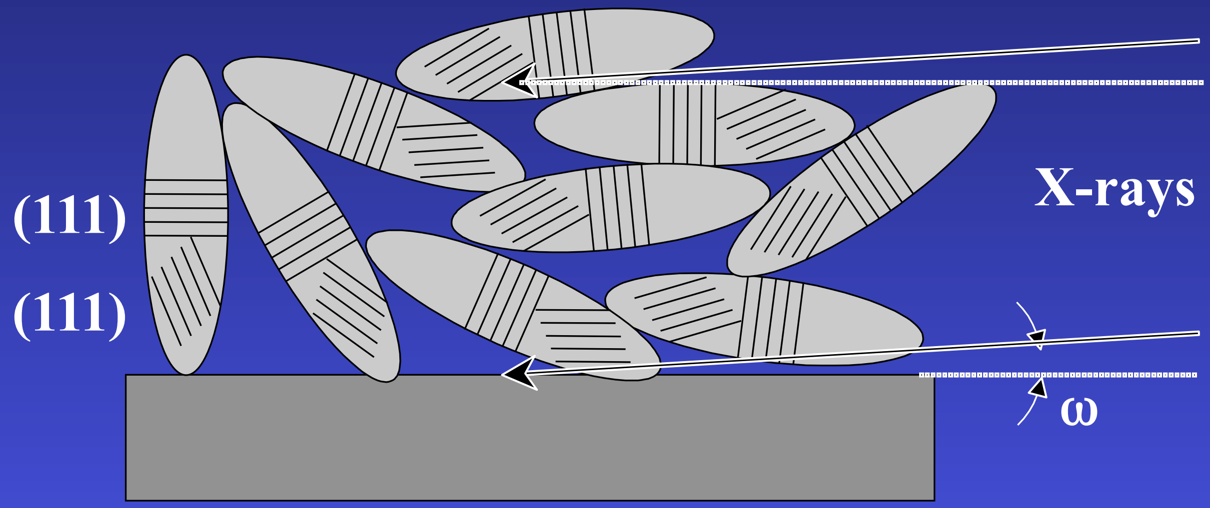

Textured

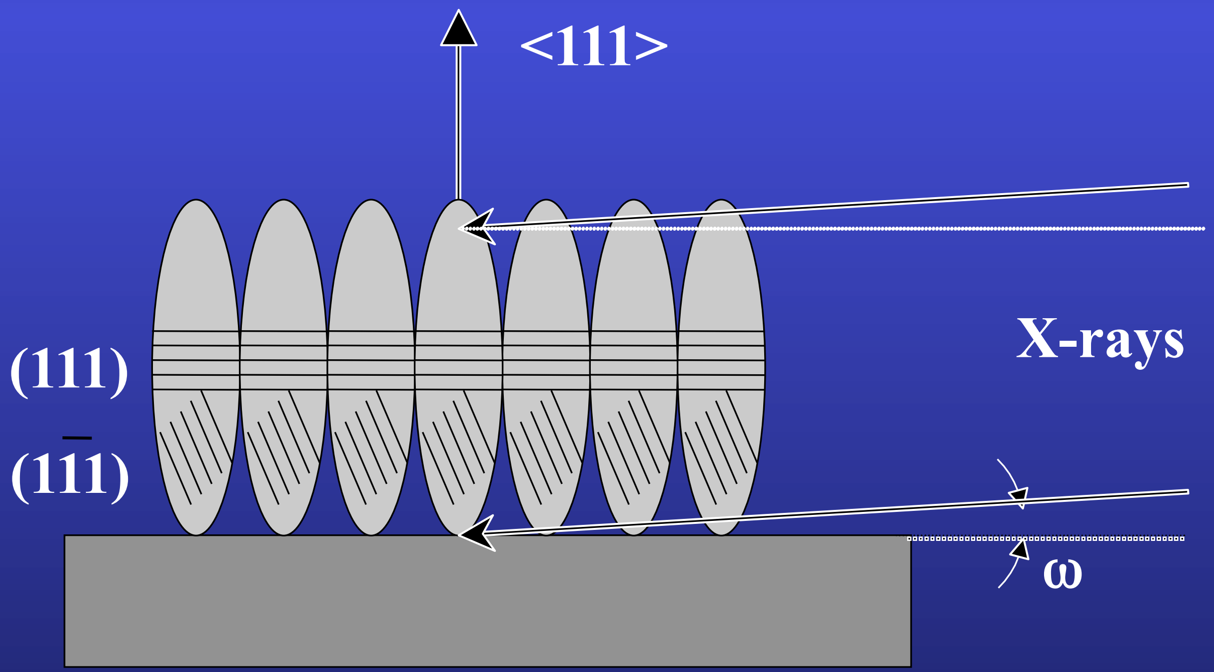

Typical refinement

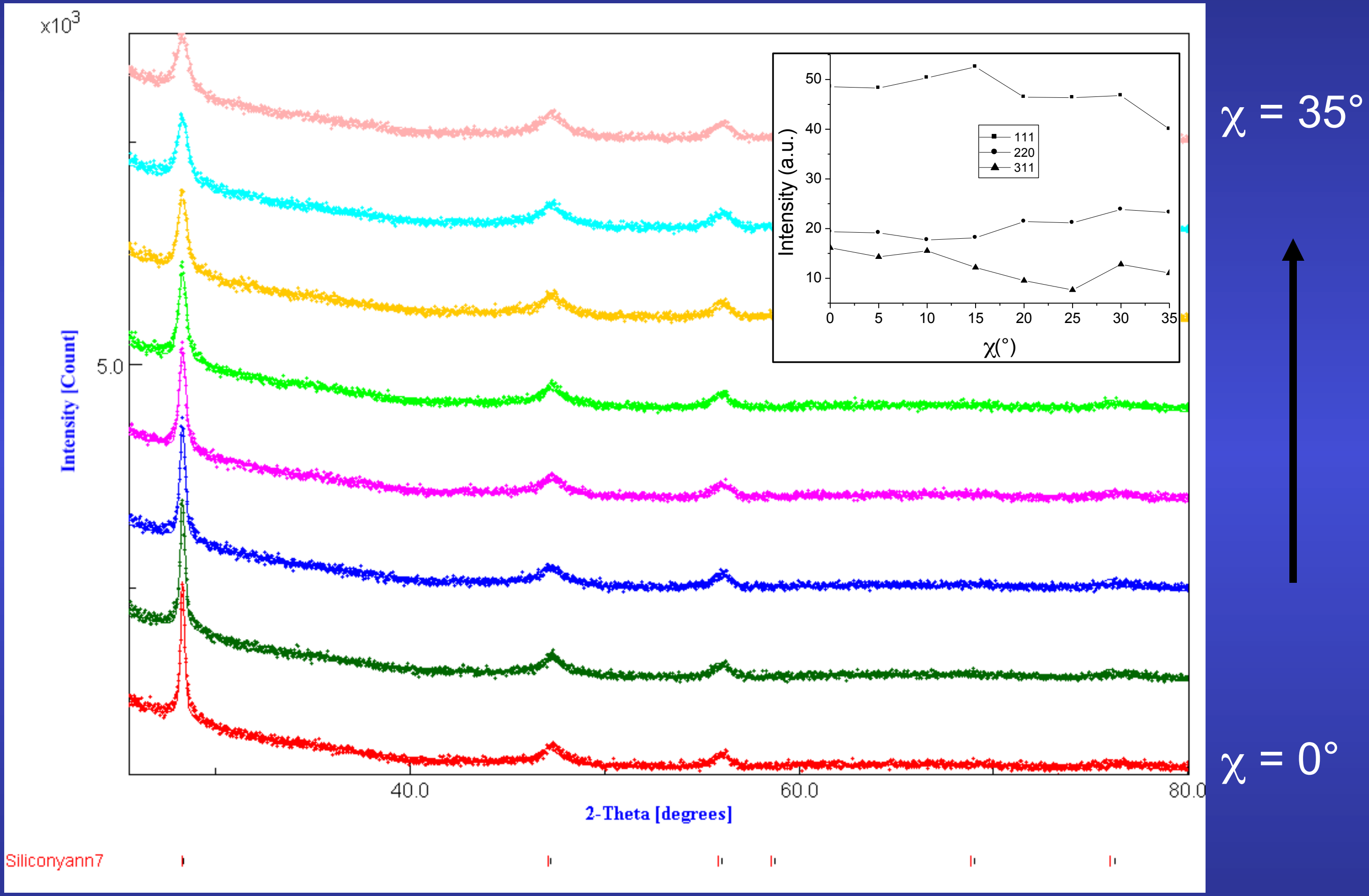

broad, anisotropic diffracted lines, textured samples

Refinement Results

Sample	d (cm)	a (Å)	RX thickness (nm)	Anisotropic sizes (Å)			Texture parameters			Reliability factors (%)			
				<111>	<220>	<311>	Maximum (m.r.d.)	minimum (m.r.d.)	Texture index F^2 (m.r.d^2)	RP_0	R_w	R_B	R_{exp}
A	4	5.4466 (3)	---	94	20	27	1.95	0.4	1.12	1.72	4.0	3.7	3.5
B	6	5.4439 (2)	711 (50)	101	20	22	1.39	0.79	1.01	0.71	4.9	4.3	4.2
C	7	5.4346 (4)	519 (60)	99	40	52	1.72	0.66	1.05	0.78	4.3	4.0	3.9
D	8	5.4461 (2)	1447 (66)	100	22	33	1.57	0.63	1.04	0.90	5.5	4.6	4.5
E	10	5.4462 (2)	1360 (80)	98	20	25	1.22	0.82	1.01	0.56	5.0	3.9	4.0
F	12	5.4452 (3)	1110 (57)	85	22	26	1.59	0.45	1.05	1.08	4.2	3.5	3.7
G	6	5.4387 (3)	1307 (50)	89	22	28	1.84	0.71	1.01	1.57	5.2	4.7	4.2
H	12	5.4434 (2)	1214 (18)	88	22	24	2.77	0.50	1.12	2.97	5.0	4.5	4.3

Mean anisotropic shape

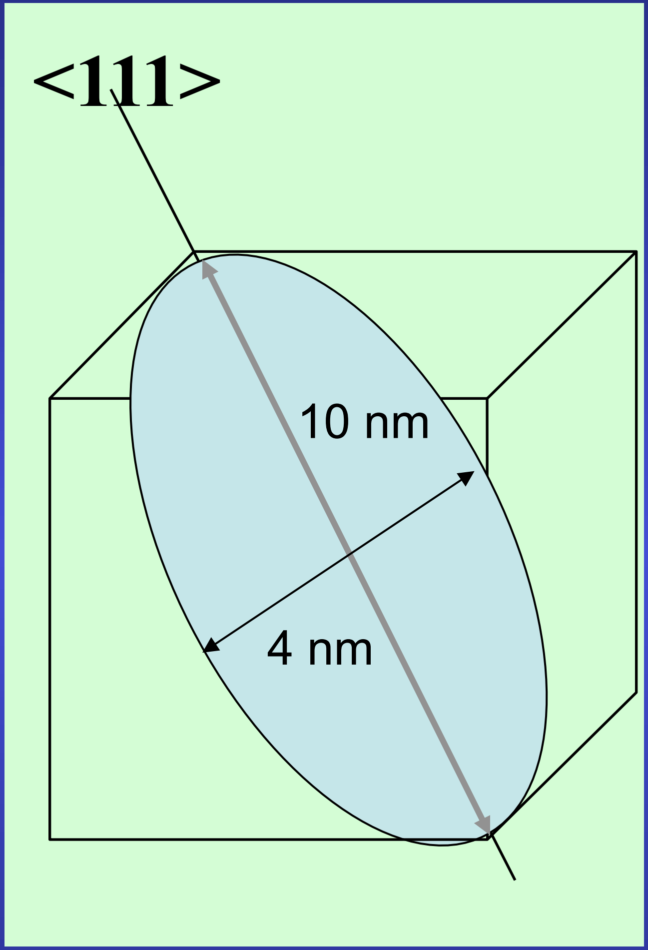

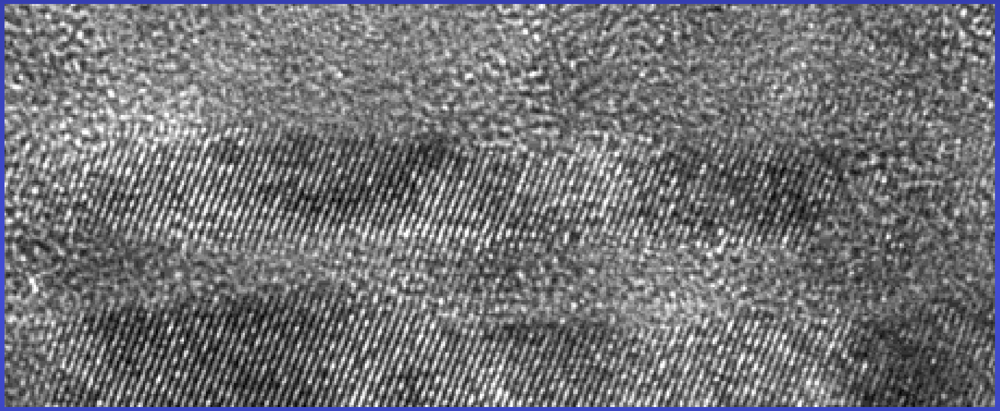

Schematic of the mean crystallite shape for Sample D represented in a cubic cell, as refined using the Popa approach and exhibiting a strong elongation along <111>, and TEM image

001 Inverse Pole Figures

a-SiO_2

(100)-Si

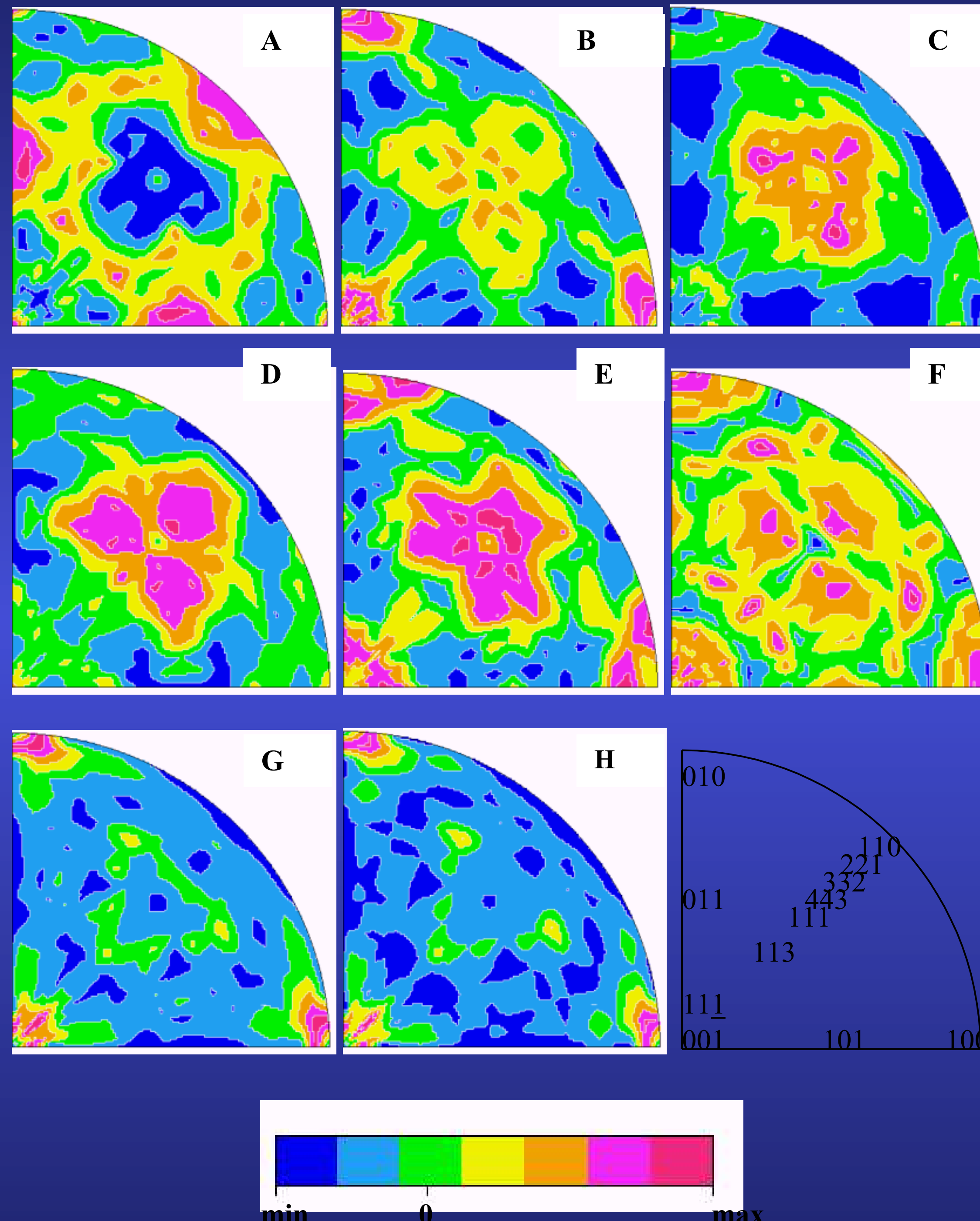

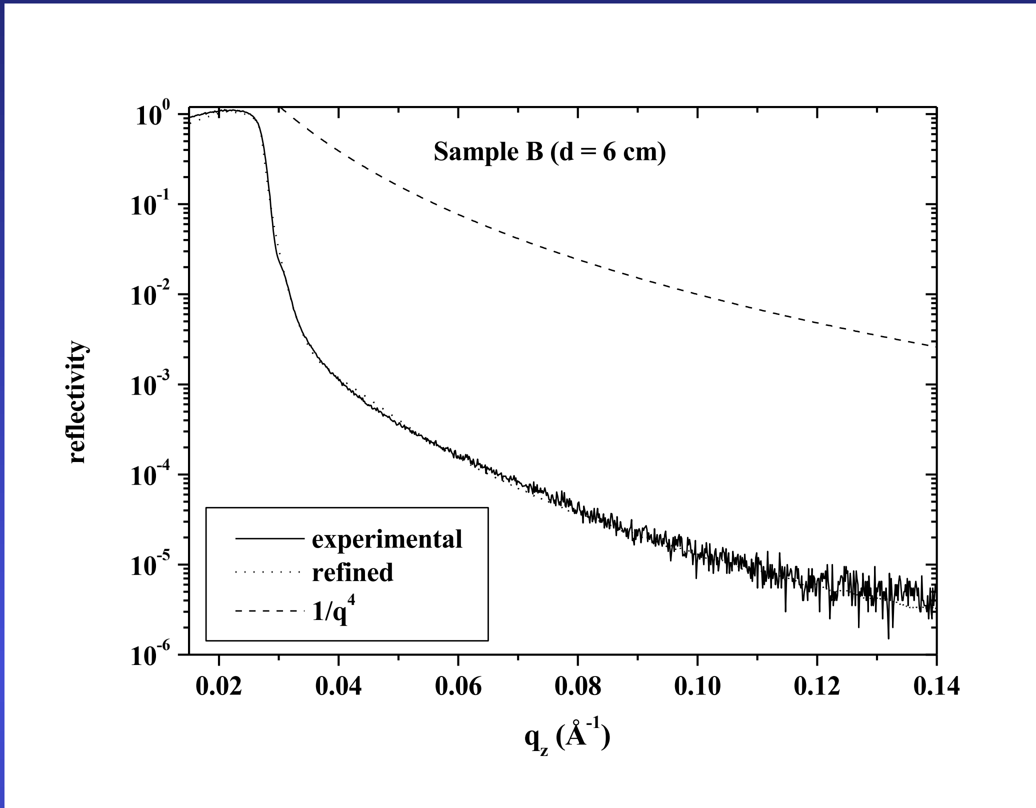

XRR:

Roughness governed

AFM:

homogeneous roughness

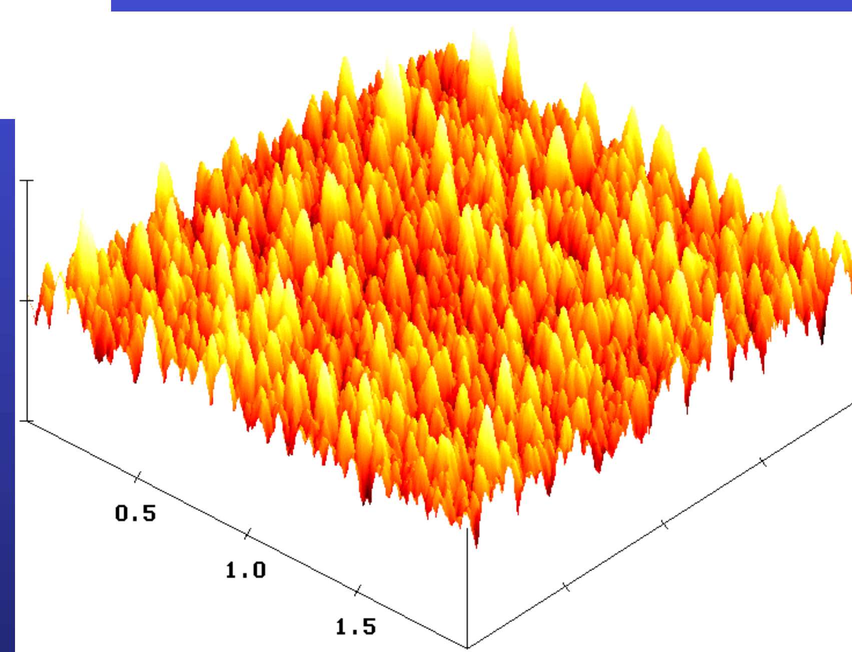

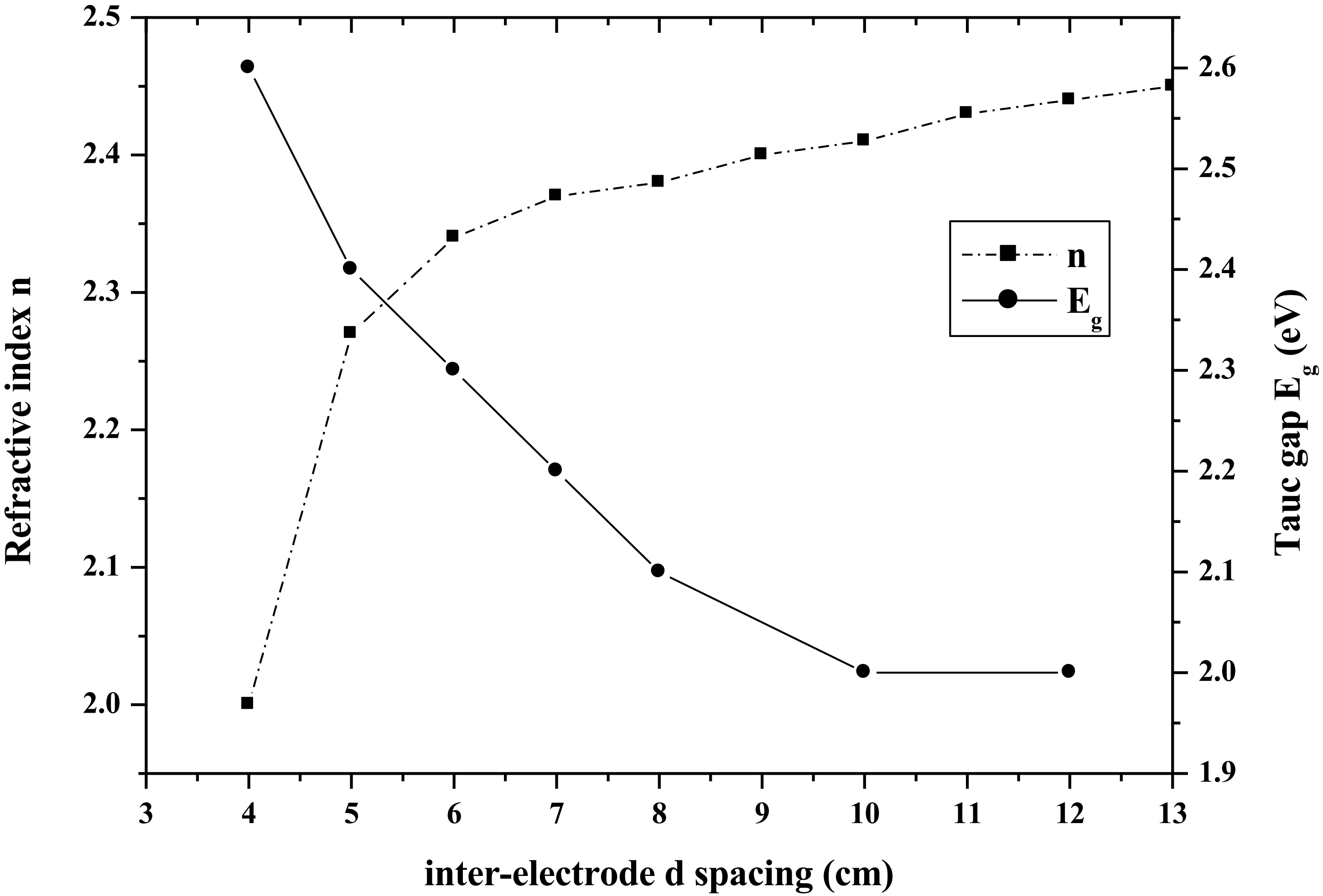

Refractive index n
Tauc gap E_g (eV)
inter-electrode d spacing (cm)
n
E_g
2.0
2.1
2.2
2.3
2.4
2.5
1.9
2.0
2.1
2.2
2.3
2.4
2.5
2.6
3
4
5
6
7
8
9
10
11
12
13

Conclusions

a) Texture affects phase ratio and structure determination

b) Microstructure (crystallite size) affects texture (go to a)

c) Stresses shift peaks then affects structure and texture determination

d) Combined analysis may be a solution, unless you can destroy your sample or are not interested in macroscopic anisotropy ...

e) If you think you can destroy it, perhaps think twice

f) more information is always needed: local probes …

g) www.ecole.ensicaen.fr/~chateign/texture/combined.pdf